

Article

Development of a ZTD Vertical Profile Model Considering the Spatiotemporal Variation of Height Scale Factor with Different Reanalysis Products in China

Xin Wang¹, Ge Zhu¹, Liangke Huang^{1,*}, Haoyu Wang^{1,*}, Yunzhen Yang², Junyu Li¹, Ling Huang¹, Lv Zhou¹ and Lilong Liu¹

¹ College of Geomatics and Geoinformation, Guilin University of Technology, Guilin 541004, China

² College of Resources and Environment, Beibu Gulf University, Qinzhou 535011, China

* Correspondence: lkhuang@whu.edu.cn (L.H.); haoyu@glut.edu.cn (H.W.)

Abstract: Tropospheric delay is one of the key factors that may affect high-precision satellite navigation and positioning and water vapor retrieval performance. Its variation in the vertical direction is much greater than that in the horizontal direction. Therefore, the vertical profile model of zenith total delay (ZTD) is important for the spatial interpolation of high-precision ZTD products and the development of ZTD models. However, in China, low spatial and temporal resolutions remain persistent in ZTD vertical profile models and limit their application. In this study, ZTD vertical profile grid models (CZTD-H model: CZTD-HM and CZTD-HE models) were developed by considering the time-varying height scale factor for China and employing ZTD layered profile information with high temporal-spatial resolution calculated using MERRA-2 data and ERA5 data based on the integration method during 2012–2016. The CZTD-H model accuracy was verified using the global navigation satellite system (GNSS) data acquired from the Crustal Movement Observation Network of China (CMONOC) and radiosonde data as reference and was compared with the canonical GPT3 model accuracy. The applicability of CZTD-HM and CZTD-HE models was discussed. The results showed that: (1) CZTD-HM and CZTD-HE models exhibited excellent performance for ZTD layered vertical interpolation in northwestern and southeastern China, respectively. Among ZTD layered profiles from 84 radiosonde stations, the RMSE of ZTD data interpolated using CZTD-HM and CZTD-HE models improved by 12.9/16.23% and 13.8/17.16% compared with GPT3-1 and GPT3-5 models, respectively. (2) The CZTD-H model maintained high performance for the spatial interpolation of GGOS grid ZTD data. Validation with ZTD data from 249 GNSS stations showed that the RMSEs of both CZTD-HM and CZTD-HE models improved by 2.8 mm (19.7%) and 2.6 mm (18.6%) compared with those of the GPT3-1 and GPT3-5 models, respectively. The CZTD-HE model showed excellent performance in summer among all the models. Only the location and day of the year were required for the application of the CZTD-H model, which showed excellent ZTD vertical correction performance in China. With the different performances of the CZTD-HE and CZTD-HM models in China, the ERA5 model can be recommended for practical applications. Therefore, these results can provide a reference for the data source selection of ZTD vertical profile model construction on the basis of high-precision reanalysis data, GNSS real-time high-precision positioning, and GNSS meteorology in China.

Keywords: zenith total delay; tropospheric delay model; vertical stratification; height scale factor; China



Citation: Wang, X.; Zhu, G.; Huang, L.; Wang, H.; Yang, Y.; Li, J.; Huang, L.; Zhou, L.; Liu, L. Development of a ZTD Vertical Profile Model Considering the Spatiotemporal Variation of Height Scale Factor with Different Reanalysis Products in China. *Atmosphere* **2022**, *13*, 1469. <https://doi.org/10.3390/atmos13091469>

Academic Editor: Doris Folini

Received: 31 July 2022

Accepted: 6 September 2022

Published: 9 September 2022

Publisher's Note: MDPI stays neutral with regard to jurisdictional claims in published maps and institutional affiliations.



Copyright: © 2022 by the authors. Licensee MDPI, Basel, Switzerland. This article is an open access article distributed under the terms and conditions of the Creative Commons Attribution (CC BY) license (<https://creativecommons.org/licenses/by/4.0/>).

1. Introduction

Tropospheric delay, which refers to signal delay caused by electromagnetic signals passing through the neutral atmosphere at an altitude of <50 km, is an essential factor in satellite navigation. In the zenith direction, the tropospheric delay may be approximately 2 m and can increase to 20 m with a decrease in the satellite altitude angle [1,2]. High-precision initial tropospheric delay information can greatly reduce the convergence time

of precise point positioning (PPP) and considerably improve the accuracy of elevation component estimation, especially in global navigation satellite system (GNSS) PPP [3–6]. And zenith tropospheric delay (ZTD) is also a key factor in GNSS water vapor retrieval. In recent years, ZTD derived from atmospheric reanalysis data has been widely applied to GNSS real-time and high-precision positioning as well as GNSS water vapor inversion [7–10]. However, in China, substantial height differences occur because of the highly fluctuant terrain. Due to the inconsistent height between the grid points of atmospheric reanalysis data and GNSS users, especially in western China at the position of GNSS users, the tropospheric delay information must be obtained through spatial interpolation with a high-precision tropospheric vertical profile model. Therefore, high-precision and real-time and ZTD vertical profile models must be studied in China.

Current tropospheric models are based on observed meteorological parameters and empirical analyses. Models requiring the observed meteorological parameters mainly include Hopfield [11], Saastamoinen [12], and Black models [13]. The application of such models in real-time vertical tropospheric correction remains challenging because the meteorological parameters measured at GNSS user locations are not easy to obtain in real-time. Therefore, several regional or global real-time tropospheric models, such as the UNB series models [14], and the EGNOS model [15] have been proposed. These models highly depend on the meteorological parameters at the sea level. They exhibit a good correction effect but have some limitations. For example, a low temporal-spatial resolution is observed in their meteorological parameters. So, some refined tropospheric models based on the reanalysis data have been proposed, such as the GPT series models, which are developed by the reanalysis data from European Centre for Medium-Range Weather Forecasts (ECMWF). In GPT series models, the GPT2w model was improved by Bohm et al. on the basis of the GPT2 model and was widely applied in the study of GNSS meteorology [16]. The latest GPT3 model was proposed in recent years [17]. Compared with the GPT2 model, GPT2w and GPT3 models not only show the improved horizontal resolution of model parameters but also provide other information. And in real-time precise tropospheric corrections, some studies focus on the joint use of GNSS and numerical weather prediction (NWP) data to maximize its advantages. For example, Zhang et al. [18] proposed real-time wide-area precise tropospheric corrections (WAPTCS) for China based on the GNSS-ZTDs and NWP-ZTDs, which has better performance than the conventional models in the tropospheric delay domain.

Due to the extensive use of reanalysis data in tropospheric correction, the development of tropospheric vertical tropospheric profile models has been widely concerned, and many global or regional tropospheric delay models have been established. The tropospheric vertical profile model is mainly expressed using the quadratic polynomial [19], highly grid model [20,21], and negative exponential function [22–27]. The ZTD vertical profile function is the key factor for developing a vertical profile model and obtaining high-precision ZTD information. Moreover, various functions, such as linear, exponential, and Gaussian functions, have been developed for ZTD vertical stratification [16,17,19]. These models present excellent performance in tropospheric vertical correction, but the spatial resolution of their parameters is low. Therefore, global tropospheric vertical profile models with high spatial resolution have been developed using atmospheric reanalysis data [28–32], and these models achieve a good result. For example, Hu et al. [29] combined the monthly mean ZTD data from ERA-Interim data of ECMWF to develop a ZTD vertical profile model based on seasonal Gaussian function. Huang et al. [33] developed a ZTD vertical profile model based on the second Modern-Era Retrospective analysis for Research and Applications (MERRA-2) data and a sliding window algorithm method. However, the accuracy and applicability of tropospheric vertical profile models based on different high-precision atmospheric reanalysis data should be further and comprehensively studied.

Although these tropospheric vertical profile models present unique advantages, a ZTD vertical profile model with excellent all-around performance remains unavailable in China. Due to large topographic fluctuations and complex climate in China, especially in western

China, a tropospheric vertical profile model that considers the fine space-time characteristics of the tropospheric height scale factor must be urgently established to meet the requirements of real-time and high-precision tropospheric vertical correction. Therefore, we proposed a method to develop a ZTD vertical-profile grid model (CZTD-H model) by considering the time-varying height scale factor on the basis of high-resolution reanalysis data for China. The layered ZTD profile information obtained from the integral calculation of MERRA-2 reanalysis data provided by the National Aeronautics and Space Administration (NASA) and the fifth generation Global Climate Reanalysis dataset (ERA5) operated by ECMWF were used to develop CZTD-HM and CZTD-HE models, respectively. The spatial interpolation performance of these two models was verified using radiosonde (RS) data acquired for China and GNSS data obtained from the Crustal Movement Observation Network of China (CMONOC) as reference values, and the applicability of these models was compared and studied with GPT3 model. The research results can provide crucial references for real-time and high-precision satellite positioning and GNSS water vapor detection in China.

2. Data and Methodology

2.1. Data Description

The research data used in this paper include MERRA-2 and ERA5 reanalysis, radiosonde (RS), GNSS, and global geodetic observing system (GGOS) atmospheric grid ZTD data. MERRA-2 and ERA5 reanalysis data acquired from 2012 to 2016 were used to establish CZTD-HM and CZTD-HE models. CZTD-HM, CZTD-HE, and GPT3 models were evaluated using RS ZTD, GNSS ZTD, and GGOS ZTD data.

2.1.1. Reanalysis Products

MERRA-2 is the latest generation of atmospheric reanalysis data provided by NASA, with horizontal spatial and temporal resolutions of $0.625^\circ \times 0.5^\circ$ (longitude \times latitude) and 6 h, respectively (<https://goldsmr4.gesdisc.eosdis.nasa.gov/data/MERRA2/> accessed on 1 January 2022). ERA5 is the (<https://cds.climate.copernicus.eu/cdsapp#!/search?text=ERA5> accessed on 1 January 2022) latest generation reanalysis data of ECMWF. Its horizontal spatial and temporal resolutions are $0.25^\circ \times 0.25^\circ$ (longitude \times latitude) and 1 h, respectively. For MERRA-2 and ERA5 reanalysis data, each grid point comprises 42 and 37 layers of data distributed according to standard pressure layers. Jiang et al. [34] and Huang et al. [35] have systematically evaluated the performance of ZTD data obtained from ERA5 and MERRA-2, respectively. The mean bias and root mean square (RMS) of ERA5 and MERRA-2 layered ZTD data are approximately 2.97/5.3 and 11.49/16.1 mm, respectively. Thus, ERA5 and MERRA-2 ZTD present a high accuracy in China. In this study, the integral method was used for calculating the ZTD value of MERRA-2 and ERA5 data acquired during 2012–2016.

2.1.2. Radiosonde Data

RS data are available for free to download from the upper-air archive on the website of the University of Wyoming (<http://weather.uwyo.edu/upperair/sounding.html> accessed on 1 January 2022). Currently, more than 1500 RS stations are available worldwide. Each RS station provides the stratified data of meteorological and surface parameters, such as precipitable water vapor (PWV) from the surface to near-earth space of approximately 30 km. All the atmospheric stratification profile data obtained from the RS station include the measured values and are one of the most reliable atmospheric stratification data. RS data can be used to calculate zenith statics delay (ZHD)/zenith wet delay (ZWD)/ZTD stratified profiles by using the same integration method as ZTD retrieval from reanalysis products. In this study, the ZHD/ZWD/ZTD stratified profiles of each RS station were calculated at UTC 00:00 and UTC 12:00 by employing the data from 84 RS stations, and then, the vertical correction accuracy of the developed model was tested using these RS ZTD. The distribution of RS stations is shown in Figure 1.

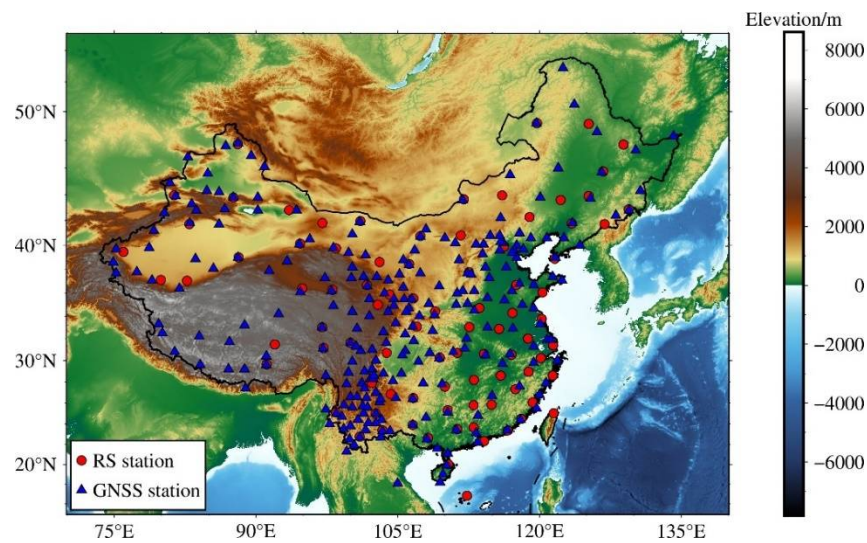


Figure 1. Distribution of selected GNSS and RS stations in China.

2.1.3. GNSS ZTD

GNSS ZTD was obtained from the crustal movement observation network (CMONOC) with a time resolution of 1 h. The ZTD product of CMONOC is generated using GAMIT/GLOBK software to process the original GNSS observation data by using the network solution, which has high precision and reliability. In this study, ZTD products from 249 GNSS stations in China were selected as references to evaluate the spatial interpolation accuracy of the established model. The distribution of GNSS stations is shown in Figure 1.

2.1.4. GGOS Atmosphere Grid ZTD Data

The GGOS atmosphere product (<https://vmf.geo.tuwien.ac.at> accessed on 1 January 2022) was acquired from the Austrian Science fund “GGOS Atmosphere Project” performed by the Vienna University of Technology. The atmospheric delay products of GGOS include the global grid products and tropospheric atmospheric parameter information of the Global International GNSS Service (IGS), very long baseline interferometry (VLBI), and other stations. In this study, spatial interpolation performance for grid products that use the developed model was tested by employing the GGOS atmosphere grid ZTD data in China, with horizontal and temporal resolutions of $1^\circ \times 1^\circ$ (longitude \times latitude) and 6 h, respectively.

2.2. Methods

2.2.1. The Method of Calculating ZTD

The vertical profile of ZTD at each grid point can be determined by integrating the refractivity at each layer height. And the atmospheric refractivity is calculated from the meteorological parameters of each layer. The specific formula is as follows [33,36]:

$$ZTD = 10^{-6} \int_{h_L}^{h_{top}} N dh \tag{1}$$

$$ZWD = 10^{-6} \int_{h_L}^{h_{top}} N_w dh \tag{2}$$

$$ZTD = ZHD + ZWD \tag{3}$$

$$N = k_1 \frac{(P - e)}{T} + k_2 \frac{e}{T} + k_3 \frac{e}{T^2} \tag{4}$$

$$N_w = k'_2 \frac{e}{T} + k_3 \frac{e}{T^2} \tag{5}$$

$$e = \frac{Sh \times P}{0.622} \tag{6}$$

where N is the total refractivity, N_w is the wet refractivity, h_L and h_{top} are the lowest and topmost height calculated by atmospheric data integration, respectively, P is the atmospheric pressure (hPa), e is the water vapor pressure (hPa), T is the temperature (K), h is the height (m), k_1, k_2, k'_2, k_3 are both the refractive index and they are 77.604 K/hPa, 64.79 K/hPa, 22.97 K/hPa, and 375,463 K²/hPa, respectively, Sh is the specific humidity.

Since there is only tropospheric ZHD at the top pressure level, to improve the integration accuracy of ZTD, the Saastamoinen model is used to calculate the atmospheric residual ZHD value at the top of the reanalysis data, which is attached to the integration results of each layer.

$$ZHD_{top} = \frac{0.0022767 \cdot P_{top}}{1 - 0.002667 \cdot \cos(2\varphi) - 0.0000028 \cdot h_{top}} \tag{7}$$

where ZHD_{top} is the ZHD above the top pressure level, P_{top} is the top atmospheric pressure (hPa), and φ is the latitude ($^\circ$).

2.2.2. The Method of Calculating ZTD Height Scale Factor

For the tropospheric vertical profile, a negative exponential function is usually adopted to express the vertical variation of the troposphere [20–23] and achieve a good vertical correction effect of the troposphere. Therefore, the ZTD vertical profile was achieved using the negative exponential function in this study. Its expression is as follows:

$$ZTD_t = ZTD_0 \cdot \exp(\beta \cdot H_1) \tag{8}$$

where ZTD_t represents the ZTD value at the target altitude H_t , ZTD_0 represents the surface ZTD value (unit: m), β is the model parameter (unit: km), H_1 is the elevation (unit: km).

So, the ZTD at positions A and B can be expressed by Equations (9) and (10) respectively, and Equation (11) can be derived.

$$ZTD_A = a_1 \cdot \exp(\beta \cdot H_a) \tag{9}$$

$$ZTD_B = a_1 \cdot \exp(\beta \cdot H_b) \tag{10}$$

$$ZTD_A = ZTD_B \cdot \exp(\beta \cdot (H_a - H_b)) \tag{11}$$

Since β is small, for convenience, we convert it through Equation (12).

$$H_s = -\frac{1}{\beta} \tag{12}$$

Equation (11) can be rewritten as:

$$ZTD_A = ZTD_B \cdot \exp\left(-\frac{H_a - H_b}{H_s}\right) \tag{13}$$

where ZTD_A and ZTD_B represent the ZTD value at the positions A and B, a_1 and β are the model parameters, H_a and H_b are the elevation at positions A and B, and H_s is the ZTD height scale factor (unit: km).

3. Development of the ZTD Vertical Profile Model Considering the Time-Varying Height Scale Factor

3.1. Analysis of the ZTD Height Scale Factor

To analyze the spatial and temporal characteristics of H_s , four MERRA-2 grid point data were selected and their time series of daily H_s during 2012–2016 was calculated. Then, H_s was fitted through the cosine function of annual and semi-annual periods, and the periodic change of H_s was analyzed using fast-Fourier transform (FFT). The results are shown in Figures 2 and 3. H_s shows considerable seasonal variations, which are mainly manifested as annual and semi-annual cycles (Figures 2 and 3). The evident characteristics

of annual and semi-annual cycles are shown in the low-latitude region, and the middle-latitude area presents more considerable annual cycle changes than semi-annual cycle changes. The annual mean value and annual and semi-annual period amplitudes of H_s were calculated for each grid of MERRA-2 and ERA5 data in China during 2012–2016 to analyze the distribution characteristics of H_s . The results are shown in Figure 4. The large annual mean values of H_s resulting from large topographic fluctuations can be observed in western China. The annual amplitude presents an obvious latitude-related trend, that is, a large amplitude is obtained at low and high latitudes, and a small amplitude is acquired at middle latitudes. The semi-annual amplitude is larger in southwestern and northeastern China. Therefore, the annual and semi-annual cycle change of H_s should be carefully addressed during the establishment of the ZTD vertical model for China.

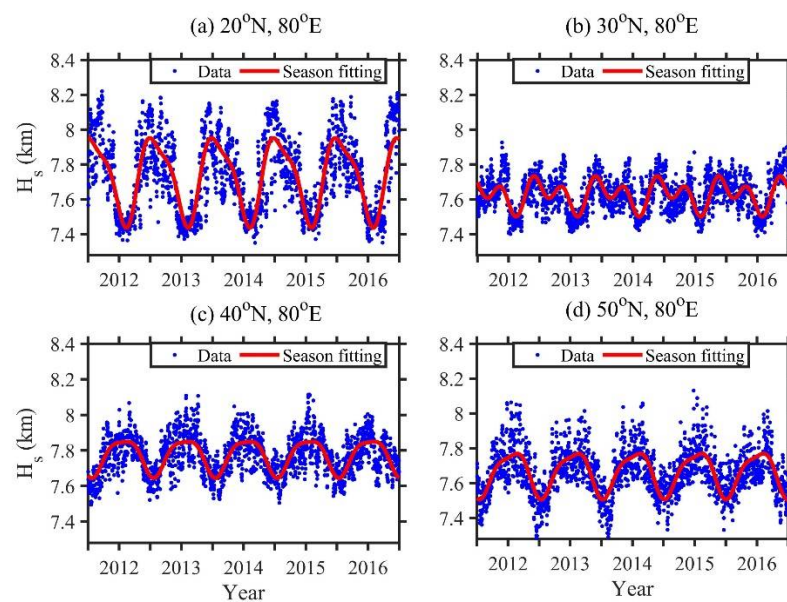


Figure 2. Time series for the ZTD height scale factor (H_s) and corresponding seasonal fits.

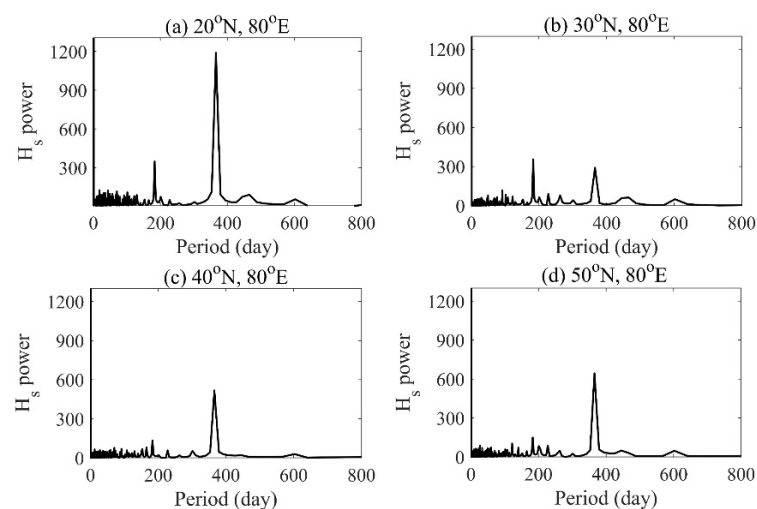


Figure 3. Time series results of periodicity detection acquired using the fast-Fourier transform algorithm.

3.2. Establishment of the CZTD-H Model

The analysis presented in Section 3.1 indicates that H_s shows important spatial-temporal characteristics in China; thus, the fine spatial-temporal variation in H_s should be considered in a model. A grid with the same horizontal resolution as the reanalysis data was selected to develop the ZTD vertical profile grid model with a high horizontal

resolution. For each grid point (15–55° N, 70–135° E) covering China, the ZTD vertical profile model can be expressed as follows:

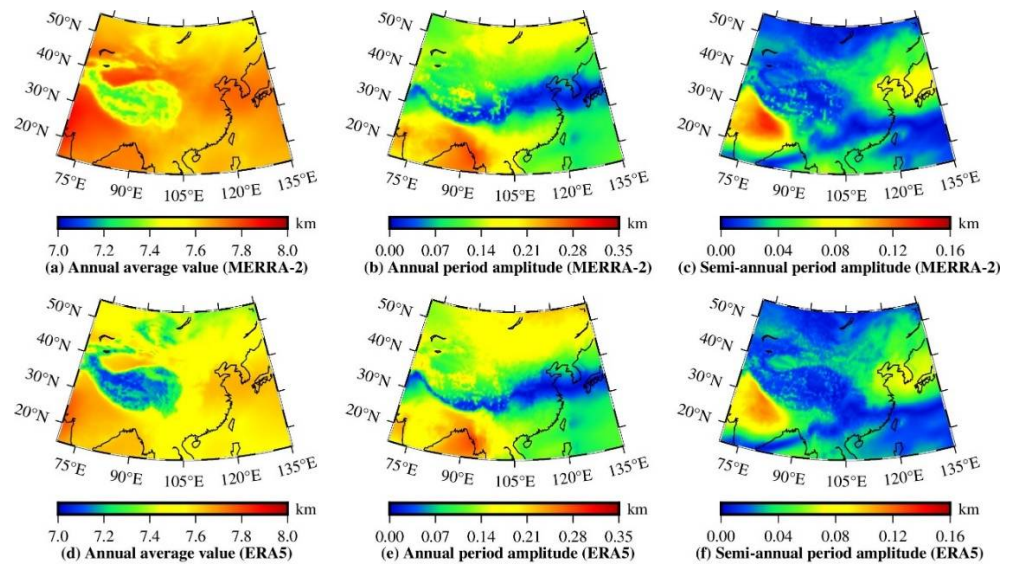


Figure 4. Distributions of the ZTD height scale factor: (a,d) annual mean (unit: mean value/km), (b,e) annual amplitude (unit: amplitude/km), and (c,f) semiannual amplitude (unit: amplitude/km).

$$ZTD_t = ZTD_r \times \exp\left(-\frac{H_t - H_r}{H_s^i}\right) \tag{14}$$

where i represents the number of grid outlets. For each grid point, the following formula can be used to describe H_s due to evident annual and semiannual cycles of H_s in China:

$$H_s^i = \beta_0^i + \beta_1^i \cos\left(2\pi \frac{DOY}{365.25}\right) + \beta_2^i \sin\left(2\pi \frac{DOY}{365.25}\right) + \beta_3^i \cos\left(4\pi \frac{DOY}{365.25}\right) + \beta_4^i \sin\left(4\pi \frac{DOY}{365.25}\right) \tag{15}$$

where DOY represents the day of the year, β_0^i is the annual mean value of the grid point i , and (β_1^i, β_2^i) and (β_3^i, β_4^i) are the annual and semi-annual periodic amplitude coefficients of grid point i , respectively.

Therefore, based on the reanalysis of grid data for China obtained during 2012–2016, the ZTD layered data of each grid point was calculated using the integral method. Then, combining Equations (8)–(13), a negative exponential function was used to express the ZTD vertical profile information of each grid point. Based on the H_s data from the ZTD vertical profile, the model coefficient of H_s was solved through least-squares adjustment, and the ZTD vertical profile grid model named CZTD-H was developed. Two variants of the CZTD-H model were established in this study: CZTD-HM and CZTD-HE. These two models primarily differ in the data source. The CZTD-HM and CZTD-HE models employ MERRA-2 ZTD and ERA5 ZTD data, respectively. For the comparison of different tropospheric vertical-profile models, ERA5 reanalysis data were resampled to obtain grid data with the horizontal and time resolution of $0.5^\circ \times 0.5^\circ$ (longitude \times latitude) and 6 h (UTC 00:00, 06:00, 12:00, and 18:00), respectively; these data are similar to MERRA-2 reanalysis data.

The model is considerably easy to use, and the process is as follows: (1) A user is only required to provide the DOY and location information of the target point. According to the location information of the target point (user), the nearest model parameter of the grid point is found, and then, H_s model parameters are obtained. (2) Based on the user’s elevation information, the ZTD value of the target point at the reference elevation can be vertically corrected to the target elevation according to Equations (14) and (15).

4. Validation and Comparison of CZTD-HM and CZTD-HE Models

The ZTD vertical correction accuracy obtained using the CZTD-H model was tested by employing RS data. The spatial interpolation accuracy of the CZTD-H model was verified using GNSS ZTD data acquired from 249 GNSS stations and GGOS grid point data. The performance of the CZTD-H model was evaluated and compared with that of the GPT3 model. The applicability of and difference between CZTD-HM and CZTD-HE models were further analyzed. The GPT3 model parameters of two horizontal resolution grids ($1^\circ \times 1^\circ$ and $5^\circ \times 5^\circ$) are represented as GPT3-1 and GPT3-5 models, respectively, in the subsequent description.

The bias and RMSE were used to evaluate the model’s accuracy. They can be calculated using the following equations:

$$\text{Bias} = \frac{1}{N} \sum_{i=1}^N (X_{O_i} - X_{R_i}) \tag{16}$$

$$\text{RMSE} = \sqrt{\frac{1}{N} \sum_{i=1}^N (X_{O_i} - X_{R_i})^2} \tag{17}$$

where N is the number of the ZTD samples, X_{O_i} and X_{R_i} are the i -th ZTD values calculated using the model and used as the reference value.

4.1. ZTD Spatial Interpolation Method

For the vertical correction of the ZTD value, ZTD vertical profile (CZTD-H model) and GPT3 models can be used to obtain the ZTD value at the target elevation. For the spatial interpolation of ZTD grid products, the interpolation method is presented below. First, based on CZTD-H and GPT3 models, the ZTD values of the four GGOS grid points nearest to GNSS stations were calculated and corrected vertically from grid points to GNSS stations. Second, after vertical correction, the ZTD values of these nearest four grid points were interpolated through bilinear interpolation, and then, the ZTD values of GGOS atmospheric grid data at each GNSS station were obtained.

The GPT3 model cannot directly provide ZTD vertical-profile model parameters. So, the ZHD and ZWD vertical profile information should be calculated on the basis of the meteorological parameters provided by the GPT3 model and the model established using physical methods. In our previous study, a physical method of using the GPT3 model was established from the UNB3 model [37]; this method can be used to conduct vertical correction starting from any reference height (H_R). Therefore, in the model accuracy comparison, the vertical correction of ZTD by using the GPT3 model can be realized by combining Equations (18)–(20), and the specific derivation process can be seen in our previous article [33].

$$ZHD_t = ZHD_R \left[1 - \frac{\beta(H_t - H_R)}{T_0 - \beta H_R} \right]^{\frac{g}{R_d \beta}} \tag{18}$$

$$ZWD_t = ZWD_R \left[1 - \frac{\beta(H_t - H_R)}{T_0 - \beta H_R} \right]^{\frac{g \lambda'}{R_d \beta} - 1} \tag{19}$$

$$ZTD = ZHD + ZWD \tag{20}$$

where ZHD_t and ZHD_R represent the ZHD values at the target altitude H_t and reference height H_R , respectively; β is the temperature gradient; T_0 is the temperature in Kelvin; g is the surface acceleration of gravity, R_d represents the dry gas constant and is $287.0538 \text{ J} \cdot \text{kg}^{-1}$; ZWD_t and ZWD_R denote the ZWD values at H_t and H_R , respectively; and $\lambda' = w = 1 + \lambda$, where λ is the water vapor gradient.

4.2. Accuracy Validation in ZTD Spatial Interpolation

4.2.1. Accuracy Validation and Comparison by Using Radiosonde Data

To test the ZTD vertical interpolation accuracy of the CZTD-H model in China, 84 RS stations were selected, and the ZHD/ZWD/ZTD layered profile information of each RS station was calculated at UTC 00:00 and UTC 12:00 in 2017 by using the integral method. This information was treated as the reference value for accuracy validation. In model validation through RS profile data, the data at the surface layer of the RS station were vertically interpolated to each layer until they reached the top layer of the RS profile. Because the CZTD-H model exhibited a higher horizontal resolution than the GPT3-1 and GPT3-5 models, the parameters of CZTD-H were resampled in a similar or the same horizontal resolution as those of the GPT3 model for fair model comparison. The CZTD-HM model parameters were resampled to $1.25^\circ \times 1^\circ$ (longitude \times latitude) and $5^\circ \times 4^\circ$ (long \times lat) resolutions and denoted as CZTD-HM-1 and CZTD-HM-5 models, respectively. The CZTD-HE model parameters were resampled to $1^\circ \times 1^\circ$ (long \times lat) and $5^\circ \times 5^\circ$ (long \times lat) resolutions and denoted as CZTD-HE-1 and CZTD-HE-5 models, respectively. The accuracy of CZTD-HM and CZTD-HE models with different horizontal resolutions applied for RS ZTD vertical interpolation was tested. The results are presented in Table 1. CZTD-HM and CZTD-HE models with different horizontal resolutions exhibit a similar accuracy for the vertical interpolation of RS ZTD data (Table 1). Therefore, the accuracy of CZTD-HM and CZTD-HE models with the horizontal resolutions of $0.5^\circ \times 0.625^\circ$ (long \times lat) and $0.5^\circ \times 0.5^\circ$ (long \times lat) was used and compared with that of GPT3-1 and GPT3-5 models. The statistical results of each RS station are presented in Table 2 and Figure 5. With an average bias of -16.9 mm, whereas the positive bias of the CZTD-HE model was more obvious, with an average bias of 9.5 mm. Compared with GPT3-1 and GPT3-5 models, the absolute value of mean bias between CZTD-HM and CZTD-HE models decreased by 31.4 mm (76.8%)/ 24 mm (58.68%) and 32.3 mm (77.3%)/ 24.9 mm (59.6%), respectively. CZTD-HM and CZTD-HE models showed small RMSEs in ZTD vertical interpolation; these RMSEs were 6.9 mm (12.9%)/ 8.7 mm (16.23%) and 7.5 mm (13.8%)/ 9.3 mm (17.16%) lower than those of GPT3-1 and GPT3-5 models, respectively. The CZTD-H model showed high stability and accuracy in ZTD vertical interpolation in China.

Table 1. Error statistics of ZTD layered vertical interpolation obtained using the CZTD-H model with different spatial resolutions compared with radiosonde data in 2017 (unit mm).

Product	Spatial Resolution (Lon \times Lat)	Model	Bias			RMSE		
			Max	Min	Mean	Max	Min	Mean
MERRA-2	$0.625^\circ \times 0.5^\circ$	CZTD-HM	50.6	-24.7	9.5	60.2	31.7	46.7
	$1.25^\circ \times 1^\circ$	CZTD-HM-1	51.1	-24.4	9.4	60.4	31.7	46.7
	$5^\circ \times 4^\circ$	CZTD-HM-5	49.2	-24.2	8.8	60.2	31.7	46.6
ERA5	$0.5^\circ \times 0.5^\circ$	CZTD-HE	32.5	-51.5	-16.9	66.3	27.4	44.9
	$1^\circ \times 1^\circ$	CZTD-HE-1	32.2	-51.4	-17.2	67.4	28.0	44.9
	$5^\circ \times 5^\circ$	CZTD-HE-5	33.1	-53.2	-17.5	68.5	26.7	44.9

Table 2. Error statistics of ZTD layered vertical interpolation obtained using different models compared with radiosonde data in 2017 (unit mm).

Model	CZTD-HM		CZTD-HE		GPT3-1		GPT3-5	
	Bias	RMSE	Bias	RMSE	Bias	RMSE	Bias	RMSE
Max	50.6	60.2	32.5	66.3	-6.9	83.1	-3.0	85.0
Min	-24.7	31.7	-51.5	27.4	-79.4	25.5	-82.0	25.6
Mean	9.5	46.7	-16.9	44.9	-40.9	53.6	-41.8	54.2

Both GPT3-1 and GPT3-5 models showed considerable negative bias in the vertical interpolation of RS ZTD data, indicating that the interpolated ZTD data of the GPT3 model

was smaller than RS ZTD data (Table 2). The CZTD-H model showed obvious positive and negative bias. However, the negative bias of the CZTD-HM model was more obvious.

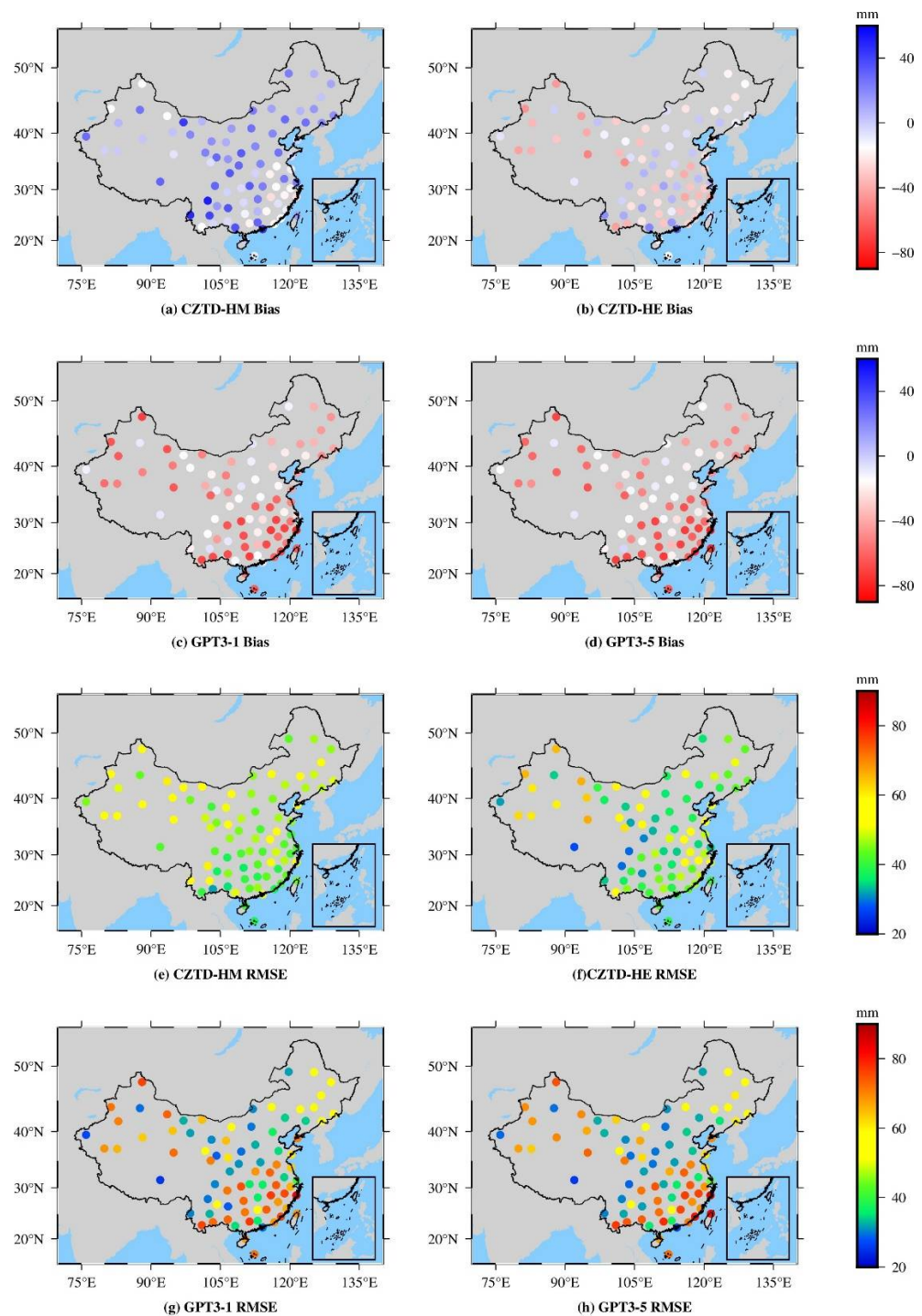


Figure 5. Distributions of the bias and RMSE of the ZTD layered vertical interpolation using different models compared with radiosonde data in 2017 for China.

The ZTD interpolation performance of various models for China is shown in Figure 5. The GPT3 model showed a negative bias in China. The CZTD-HM model exhibited a positive bias in most regions of China and a negative bias in most regions of southeast China. The CZTD-HE model showed less negative bias than the GPT3 model in most regions of China. The GPT3 model exhibited a large error in some regions of southeast and northwest China. The southeast region may be vulnerable to the strong influence of the

East Asian monsoon because of its proximity to the West Coast of the Pacific Ocean, and the water vapor content in the sea area was high and changed violently. The complex terrain and alpine climate may influence the northwest region. The CZTD-H model showed a small error in the northwest and southeast regions, which indicated a certain accuracy improvement. CZTD-HM and CZTD-HE models had higher accuracy in northwest and southeast China, respectively. In addition, the ZTD vertical interpolation accuracy of the CZTD-H model certainly improved compared with that of the GPT3-1 and GPT3-5 models in some regions of northeast China. The CZTD-HE model showed higher performance than the CZTD-HM model in eastern China. However, the CZTD-H model exhibited few improvements in central China. Compared with the GPT3 model, the CZTD-HE model had a similar accuracy, and the CZTD-HM model showed a slightly decreased accuracy for ZTD vertical interpolation in central China. In conclusion, the CZTD-HE model exhibited higher accuracy and stability than the CZTD-HM model in China. CZTD-HM and CZTD-HE models are highly suitable for northwest China and southeast and northeast China, respectively. Therefore, the combined use of multiple models can be considered for the vertical correction of ZTD.

4.2.2. Accuracy Validation and Comparison Using GNSS ZTD Data

The spatial interpolation of ZTD grid products is widely employed in GNSS atmospheric research. ZTD changes more in the vertical direction than that in the horizontal direction. Therefore, the ZTD vertical profile model is essential for obtaining excellent results from ZTD spatial interpolation. Based on the application of the GGOS ZTD grid data interpolated to GNSS sites through different models, the ZTD products obtained from 249 GNSS stations of CMONOC in 2018 were the reference values used to test the results of spatial interpolation. The accuracy statistics of the spatial interpolation of GGOS grid ZTD data are presented in Table 3 and Figure 6.

Table 3. Error statistics of spatial interpolation for GGOS gridded ZTD compared with GNSS data (unit mm).

Model	CZTD-HM		CZTD-HE		GPT3-1		GPT3-5	
	Bias	RMSE	Bias	RMSE	Bias	RMSE	Bias	RMSE
Max	14.7	25.4	21.5	26.5	71.0	72.9	63.2	64.6
Min	−14.0	4.6	−12.8	4.4	−9.5	5.6	−9.0	5.6
Mean	0.8	11.4	3.0	11.4	7.1	14.2	7.1	14.0

GPT3-1 and GPT3-5 models exhibited similar accuracy for the ZTD spatial interpolation of GGOS grid data validated through the GNSS ZTD data of CMONOC (Table 3). Compared with the GPT3 model, the CZTD-H model showed a small bias and RMSE. The mean bias of CZTD-HM and CZTD-HE models decreased by 6.3 mm (88.7%) and 4.1 mm (57.75%) compared with GPT3-1 and GPT3-5 models, respectively. The mean RMSE of CZTD-HM and CZTD-HE models decreased by 2.8 mm (19.7%) and 2.6 mm (18.6%), respectively. Both GPT3-1 and GPT3-5 models showed a small bias and RMSE in eastern China and a large bias and RMSE in western China (Figure 6). The CZTD-H model showed a small bias and RMSE in China, especially in western China, and exhibited considerable improvement compared with the GPT3 model. This may be due to the large topographic relief in the western region, which makes it difficult to accurately simulate the ZTD layered profile for the GPT3 model. Nevertheless, the GPT3 model still shows good accuracy in China. The CZTD-H model exhibited a small error and excellent performance when expressing the ZTD variation in the vertical direction, and both CZTD-HM and CZTD-HE models showed high accuracy. Furthermore, the CZTD-H model provided better results for grid ZTD spatial interpolation than the GPT3 model.

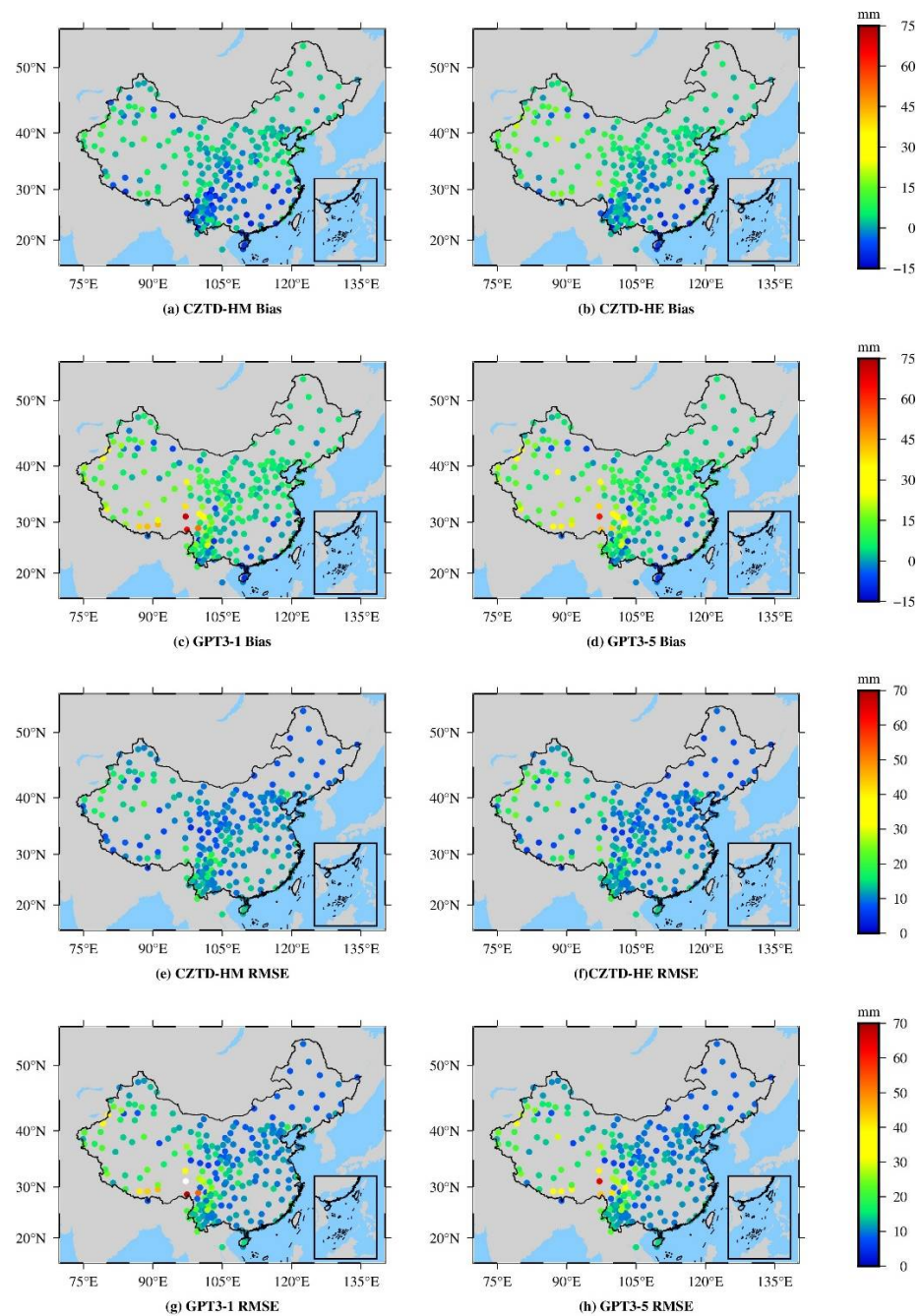


Figure 6. Distribution of bias and RMSE of spatial interpolation for GGOS gridded ZTD compared with GNSS data.

To analyze the interpolation results of each model at different heights, the heights of GNSS stations were divided into five ranges of 0 to 1, 1 to 2, 2 to 3, 3 to 4, and >4 km. The bias and RMSE were calculated (Figure 7). With the increase in the height, the bias and RMSE of GPT3-1 and GPT3-5 models gradually increased, and their accuracy decreased. The CZTD-H model showed a completely opposite trend. The RMSE and accuracy of the CZTD-H model gradually decreased and increased, respectively. Based on the RMSE value, compared with the GPT3 model, the accuracy improvement of the CZTD-H model was obvious at the height of >2 km and was substantial at the height of >4 km. At the height of >4 km, compared with that of GPT3-1 and GPT3-5 models, the RMSE of CZTD-HM and CZTD-HE models decreased by 11.2 mm (57%)/15.09 mm (77.38%) and 9.6 mm (54%)/9.13 mm (51%), respectively, in ZTD spatial interpolation. This finding

further indicated that the CZTD-H model provided excellent performance in ZTD spatial interpolation, especially in high-altitude areas. At different heights, for the bias value, the CZTD-HM model shows small values than the CZTD-HE model. For the RMSE value, the accuracy of the CZTD-HM and CZTD-HE models was similar at 1 to 2 km and considerably different at 3 to 4 km. The CZTD-HE model had good accuracy at <1 km, and the CZTD-HM model had high accuracy at >2 km. CZTD-HM and CZTD-HE models can be used to describe the changes in ZTD at different heights, which can be advantageous, and the CZTD-HM model may be more suitable at different heights in spatial interpolation.

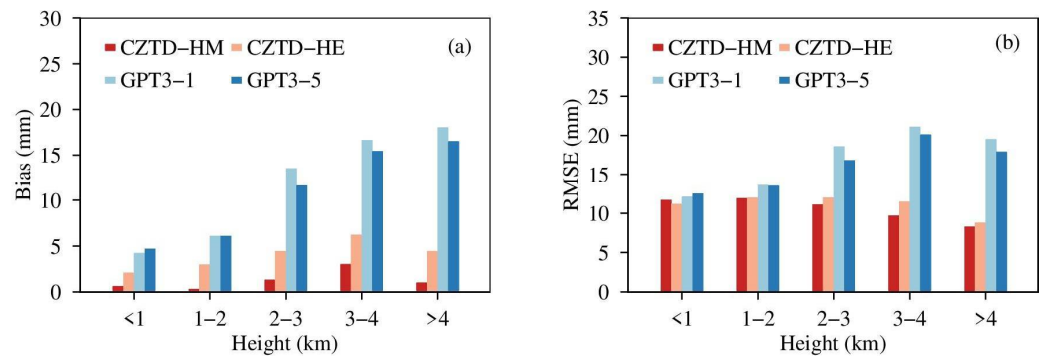


Figure 7. Bias and RMSE of spatial interpolation for GGOS gridded ZTD for CZTD-H and GPT3 models at different heights validated by GNSS data.

To analyze the seasonal variations in the bias and RMSE of different models for ZTD spatial interpolation, the monthly mean bias and RMSE of 249 GNSS stations were calculated (Figure 8). The GPT3 model showed a positive mean bias throughout the year, and the CZTD-H model exhibited a negative mean bias in summer and a positive mean bias during other seasons (Figure 8). The RMSE of CZTD-H and GPT3 models showed obvious seasonal variations. RMSE reached the maximum value in summer may be because of the climatic characteristics of summer. Monsoon climate is the main feature of China’s climate. Affected by the warm and humid airflow from the ocean, water vapor and other meteorological parameters are highly active in summer, which made accurate modeling difficult and it’s hard to accurately detect changes in ZTD, thereby affecting the model accuracy. However, the CZTD-H model showed better performance for improving the accuracy of the ZTD spatial interpolation of GGOS grid data than the GPT3 model. Therefore, the CZTD-H model presented more advantages in ZTD spatial interpolation than the GPT3 model.

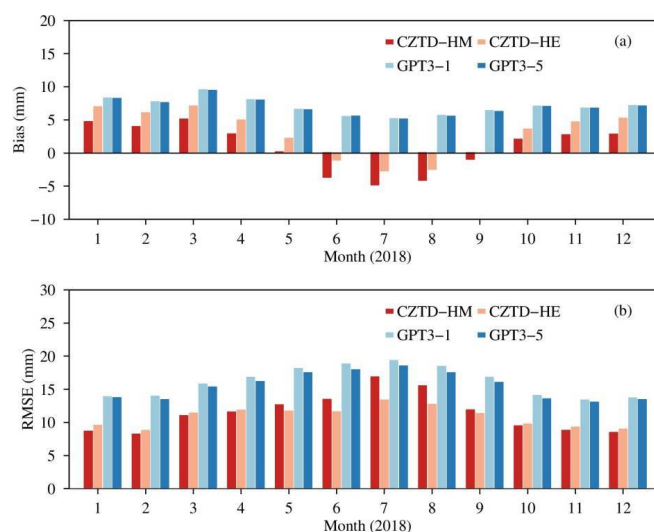


Figure 8. Bias and RMSE of spatial interpolation for GGOS gridded ZTD for CZTD-H and GPT3 models in different months validated by GNSS data.

The accuracy of CZTD-HM and CZTD-HE models showed slight differences in spring, autumn, and winter but obvious differences in summer. The CZTD-HE model showed higher performance than other models in the summer. In July, when the water vapor varied considerably, the monthly RMSE of CZTD-HM and CZTD-HE models decreased by 2.48 mm (12.78%)/5.98 mm (30.82%) and 1.64 mm (8.45%)/5.14 mm (27.69%) for spatial interpolation compared with that of GPT3-1 and GPT3-5 models, respectively. This finding may attribute to the higher spatial resolution of ERA5 reanalysis data, which facilitated the capture of changes caused by some active meteorological parameters. Simultaneously, the CZTD-HE model showed high stability and slight error fluctuations throughout the year. For spatial interpolation, the CZTD-HM model is highly suitable for spring, autumn, and winter, whereas the CZTD-HE model is highly suitable for summer.

5. Discussion and Conclusions

The ZTD vertical profile model plays a crucial role in realizing the high-precision spatial interpolation of ZTD products and developing excellent ZTD models. In this study, the ZTD vertical profile grid model (CZTD-H model) was developed for China by considering the fine seasonal variations in H_s , and the applicability of CZTD-HM and CZTD-HE models was analyzed on the basis of MERRA-2 and ERA5 data. The vertical interpolation accuracy and spatial interpolation of the CZTD-H model in China were verified using ZTD data acquired from the RS stations, GNSS stations, and GGOS grid products, and the CZTD-H model showed higher performance than the GPT3 model.

The results showed that: (1) For ZTD vertical interpolation by using RS data, the CZTD-HE model showed higher accuracy and stability than the GPT3 model, especially in northwestern and southeastern China. The CZTD-HM model was highly suitable for northwest China, whereas the CZTD-HE model was highly suitable for southeast and northeast China. (2) For ZTD spatial interpolation by GGOS grid ZTD data, the CZTD-H model showed higher accuracy and stability than the GPT3 model, especially in western China. For spatial interpolation, the CZTD-HM model was suitable at the height of >1 km and in summer, whereas the CZTD-HE model was favorable at the height of <1 km and in spring, autumn, and winter.

The CZTD-H model can provide real-time and high-precision ZTD vertical correction in China on the basis of the time information and location of users. Therefore, the CZTD-H model is easy to apply. Its good correction effect of tropospheric ZTD products helps obtain high-precision ZTD information, thereby promoting the application of atmospheric reanalysis data in GNSS studies, such as atmospheric exploration and precise positioning. However, this paper only takes a relatively comprehensive data analysis and verification to prove the stability and applicability of the developed model, and further application and improvement of the model need to be further studied. The performance of the model applied to the positioning should be discussed. The ways to expand the specific application of the model in GNSS meteorology and to extend the CZTD-H model into the ZTD vertical profile model with a comprehensive performance by combining different advantages and characteristics of multi-source reanalysis data will be the focus of our future research.

Author Contributions: Conceptualization, X.W., G.Z. and L.H. (Liangke Huang); methodology, X.W. and G.Z.; validation, X.W. and G.Z.; formal analysis, X.W., H.W. and Y.Y.; investigation, J.L., L.H. (Ling Huang) and L.Z.; writing—original draft preparation, X.W. and G.Z.; writing—review and editing, L.H. (Liangke Huang), H.W., Y.Y., J.L., L.H. (Liangke Huang), L.Z. and L.L.; funding acquisition, L.H. (Liangke Huang), J.L., L.H. (Ling Huang) and L.L. All authors have read and agreed to the published version of the manuscript.

Funding: This work was sponsored by the National Natural Foundation of China (41704027); Guangxi Natural Science Foundation of China (2020GXNSFBA297145; 2020GXNSFBA159033), the “Ba Gui Scholars” program of the provincial government of Guangxi, and the Innovation Project of Guangxi Graduate Education (grant number: YCSW2022322).

Institutional Review Board Statement: Not applicable.

Informed Consent Statement: Not applicable.

Data Availability Statement: The MERRA-2 data can be freely accessed at <https://goldsmr4.gesdisc.eosdis.nasa.gov/data/MERRA2/> accessed on 1 January 2022. The ERA5 data can be freely accessed at <https://cds.climate.copernicus.eu/cdsapp#!/search?text=ERA5> accessed on 1 January 2022. The radiosonde data can be accessed at <http://weather.uwyo.edu/upperair/sounding.html> accessed on 1 January 2022. The GGOS data can be accessed at <https://vmf.geo.tuwien.ac.at> accessed on 1 January 2022.

Acknowledgments: The authors would like to thank MERRA-2 grid data provided by NASA, ERA5 grid data provided by ECMWF, radiosonde data provided by the University of Wyoming, GNSS ZTD product provided by China Earthquake Administration, and Grid data provided by GGOS Atmosphere.

Conflicts of Interest: The authors declare no conflict of interest.

References

1. Yin, H.; Huang, D.; Xiong, Y.; Wang, G. New Model for Tropospheric Delay Estimation of GPS Signal. *Geom. Inform. Sci. Wuhan Univ.* **2007**, *32*, 454–457.
2. Zhao, J.; Song, S.; Chen, Q.; Zhou, W.; Zhu, W. Establishment of a new global model for zenith tropospheric delay based on functional expression for its vertical profile. *Chin. J. Geophys.* **2014**, *57*, 3140–3153.
3. Lu, C.X.; Li, X.X.; Zus, F.; Heinkelmann, R.; Dick, G.; Ge, M.; Wickert, J.; Schuh, H. Improving BeiDou real-time precise point positioning with numerical weather models. *J. Geod.* **2017**, *91*, 1019–1029. [[CrossRef](#)]
4. Wilgan, K.; Hadas, T.; Hordyniec, P.; Bosy, L. Real-time precise point positioning augmented with high-resolution numerical weather prediction model. *GPS Solut.* **2017**, *21*, 1341–1353. [[CrossRef](#)]
5. Zheng, F.; Lou, Y.D.; Gu, S.F.; Gong, X.; Shi, C. Modeling tropospheric wet delays with national GNSS reference network in China for BeiDou precise point positioning. *J. Geodesy* **2018**, *92*, 545–560. [[CrossRef](#)]
6. Li, H.J.; Xiao, J.X.; Zhang, S.J.; Zhou, J.; Wang, J.X. Introduction of the double-differenced ambiguity resolution into precise point positioning. *Remote Sens.* **2018**, *10*, 1779. [[CrossRef](#)]
7. Zhang, H.X.; Yuan, Y.B.; Li, W.; Zhang, B.C. A real-time precipitable water vapor monitoring system using the national GNSS network of China: Method and preliminary results. *IEEE J. Select. Top. Appl. Earth Observ. Rem. Sens.* **2019**, *12*, 1587–1598. [[CrossRef](#)]
8. Zhang, H.X.; Yuan, Y.B.; Li, W.; Ji, D.B.; Lv, M.H. Implementation of ready-made hydrostatic delay products for timely GPS precipitable water vapor retrieval over complex topography: A case study in the Tibetan Plateau. *IEEE J. Select. Top. Appl. Earth Observ. Rem. Sens.* **2021**, *14*, 9462–9474. [[CrossRef](#)]
9. Zhao, Q.Z.; Liu, Y.; Yao, W.Q.; Yao, Y.B. Hourly Rainfall Forecast Model Using Supervised Learning Algorithm. *IEEE Trans. Geosci. Remote Sens.* **2021**, *60*, 1–9. [[CrossRef](#)]
10. Huang, L.K.; Wang, X.; Xiong, S.; Li, J.; Liu, L.L.; Mo, Z.X.; Fu, B.L.; He, H.C. High-precision GNSS PWV retrieval using dense GNSS sites and in-situ meteorological observations for the evaluation of MERRA-2 and ERA5 reanalysis products over China. *Atmos. Res.* **2022**, *276*, 106247. [[CrossRef](#)]
11. Hopfield, H.S. Two-Quartic tropospheric refractivity profile for correcting satellite data. *J. Geophys. Res.* **1969**, *74*, 4487–4499. [[CrossRef](#)]
12. Saastamoinen, J. Contributions to the theory of atmospheric refraction. *Bull. Géodésique* **1972**, *105*, 279–298. [[CrossRef](#)]
13. Black, H.D. An easily implemented algorithm for the tropospheric range correction. *J. Geophys. Res.* **1978**, *83*, 1825–1828. [[CrossRef](#)]
14. Leandro, R.F.; Langley, R.B.; Santos, M.C. UNB3m_pack: A neutral atmosphere delay package for radiometric space techniques. *GPS Solut.* **2008**, *12*, 65–70. [[CrossRef](#)]
15. Penna, N.; Dodson, A.; Chen, W. Assessment of EGNOS tropospheric correction model. *J. Navig.* **2001**, *54*, 37–55. [[CrossRef](#)]
16. Böhm, J.; Moeller, G.; Schindelegger, M.; Pain, G.; Weber, R. Development of an improved empirical model for slant delays in the troposphere (GPT2w). *GPS Solut.* **2015**, *19*, 433–441. [[CrossRef](#)]
17. Landskron, D.; Böhm, J. VMF3/GPT3: Refined discrete and empirical troposphere mapping functions. *J. Geod.* **2018**, *92*, 349–360. [[CrossRef](#)]
18. Zhang, H.; Yuan, Y.; Li, W. Real-time wide-area precise tropospheric corrections (WAPTCs) jointly using GNSS and NWP forecasts for China. *J. Geod.* **2022**, *96*, 44. [[CrossRef](#)]
19. Song, S.L.; Zhu, W.Y.; Chen, Q.M.; Liou, Y.A. Establishment of a new tropospheric delay correction model over China area. *Sci. China Phys. Mech.* **2011**, *54*, 2271–2283. [[CrossRef](#)]
20. Li, W.; Yuan, Y.B.; Ou, J.K.; Li, H.; Li, Z.S. A new global zenith tropospheric delay model IGGtrop for GNSS applications. *Chin. Sci. Bull.* **2012**, *57*, 2132–2139. [[CrossRef](#)]
21. Li, W.; Yuan, Y.B.; Ou, J.K.; Chia, Y.J.; Li, Z.S.; Liou, Y.A.; Wang, N.B. New versions of the BDS/GNSS zenith tropospheric delay model IGGtrop. *J. Geod.* **2015**, *89*, 73–80. [[CrossRef](#)]

22. Huang, L.K.; Liu, L.L.; Yao, C.L. A zenith tropospheric delay correction model based on the regional CORS network. *Geod. Geodyn.* **2012**, *3*, 53–62.
23. Yao, Y.B.; He, C.Y.; Zhang, B.; Xu, C.Q. A new global zenith tropospheric delay model GZTD. *Chinese. J. Geophys.* **2013**, *56*, 2218–2227.
24. Yao, Y.B.; Hu, Y.F.; Yu, C. An improved global zenith tropospheric delay model. *Acta Geod. Et Cartogr. Sin.* **2015**, *44*, 242–249.
25. Chen, J.P.; Wang, J.G.; Wang, J.X.; Tan, W.J. SHAtrop: Empirical ZTD Model Based on CMONOC GNSS Network. *Geom. Inform. Sci. Wuhan Univ.* **2019**, *44*, 1588–1595.
26. Yao, Y.B.; Hu, Y.F.; Yu, C.; Zhang, B.; Guo, J.J. An improved global zenith tropospheric delay model GZTD2 considering diurnal variations. *Nonlinear Proc. Geoph.* **2016**, *23*, 127–136. [[CrossRef](#)]
27. Sun, J.L.; Wu, Z.L.; Yin, Z.D. A simplified GNSS tropospheric delay model based on the nonlinear hypothesis. *GPS Solut.* **2017**, *21*, 1735–1745. [[CrossRef](#)]
28. Yao, Y.B.; Hu, Y.F. An empirical zenith wet delay correction model using piecewise height functions. *Ann. Geophys.* **2018**, *36*, 1507–1519. [[CrossRef](#)]
29. Hu, Y.F.; Yao, Y.B. A new method for vertical stratification of zenith tropospheric delay. *Adv. Space Res.* **2019**, *63*, 2857–2866. [[CrossRef](#)]
30. Sun, Z.Y.; Zhang, B.; Yao, Y.B. A Global Model for Estimating Tropospheric Delay and Weighted Mean Temperature Developed with Atmospheric Reanalysis Data from 1979 to 2017. *Rem. Sens.* **2019**, *11*, 1893. [[CrossRef](#)]
31. Sun, Z.Y.; Zhang, B.; Yao, Y.B. An ERA5-based model for estimating tropospheric delay and weighted mean temperature over China with improved spatiotemporal resolutions. *Earth Space Sci.* **2019**, *6*, 1926–1941. [[CrossRef](#)]
32. Huang, L.K.; Zhu, G.; Peng, H.; Chen, H.; Liu, L.L.; Jiang, W.P. A global grid model for the vertical correction of zenith wet delay based on the sliding window algorithm. *Acta Geod. Cartogr. Sin.* **2021**, *50*, 685–694.
33. Huang, L.K.; Zhu, G.; Liu, L.L.; Chen, H.; Jiang, W.P. A global grid model for the correction of the vertical zenith total delay based on a sliding window algorithm. *GPS Solut.* **2021**, *25*, 98. [[CrossRef](#)]
34. Jiang, C.H.; Xu, T.H.; Wang, S.M.; Nie, W.F.; Sun, Z.Z. Evaluation of zenith tropospheric delay derived from ERA5 data over China using GNSS observations. *Rem. Sens.* **2020**, *12*, 663. [[CrossRef](#)]
35. Huang, L.K.; Guo, L.J.; Liu, L.L.; Huang, Y.L.; Xie, S.F.; Kang, C.L. Accuracy analysis of ZTD and ZWD calculated from MERRA-2 reanalysis data over China. *Geom. Inform. Sci. Wuhan Univ.* **2021**, (accepted). [[CrossRef](#)]
36. Thayer, G.D. An improved equation for the radio refractive index of air. *Radio Sci.* **1974**, *9*, 803–807. [[CrossRef](#)]
37. Leandro, R.F.; Santos, M.C.; Langley, R.B. UNB neutral atmosphere models: Development and performance. In Proceedings of the ION NTM 2006, Monterey, CA, USA, 18–20 January 2006; pp. 562–573.